

Turbulence attenuation by large neutrally buoyant particles

M. Cisse,¹ E.-W. Saw,¹ M. Gibert,^{2,3} E. Bodenschatz,^{4,5,6} and J. Bec¹

¹⁾Laboratoire Lagrange, Université de Nice-Sophia Antipolis, CNRS, Observatoire de la Côte d'Azur, Nice, France

²⁾Université Grenoble Alpes, Inst. NEEL, F-38042 Grenoble, France

³⁾CNRS, Inst. NEEL, F-38042 Grenoble, France

⁴⁾Max Planck Institute for Dynamics and Self-Organization, Göttingen, Germany

⁵⁾Institute for Nonlinear Dynamics, University of Göttingen, Göttingen, Germany

⁶⁾Laboratory of Atomic and Solid-State Physics and Sibley School of Mechanical and Aerospace Engineering, Cornell University, USA

Turbulence modulation by inertial-range-size, neutrally-buoyant particles is investigated experimentally in a von Kármán flow. Increasing the particle volume fraction Φ_v , maintaining constant impellers Reynolds number attenuates the fluid turbulence. The inertial-range energy transfer rate decreases as $\propto \Phi_v^{2/3}$, suggesting that only particles located on a surface affect the flow. Small-scale turbulent properties, such as structure functions or acceleration distribution, are unchanged. Finally, measurements hint at the existence of a transition between two different regimes occurring when the average distance between large particles is of the order of the thickness of their boundary layers.

Introducing impurities in a developed turbulent flow has drastic effects on the mechanisms of energy transfer and dissipation. A minute amount of polymer additives causes for instance drag reduction.¹ In such visco-elastic fluids, the coupling between the local flow and the polymers stretching can be modeled in order to quantify the exchanges between kinetic and elastic energies and to interpret turbulent drag reduction as a suppression of large velocity gradients.² The mechanisms at play in turbulent suspensions of finite-size spherical particles are much more intricate and turbulence can either be enhanced or suppressed.³ In wall flows, transition to turbulence can be either hindered or facilitated depending on the size and volume fraction of particles.^{4,5} In the case of developed turbulence, depending on the size of impurities, on their density ratio, and volume fraction, both turbulent kinetic energy and dissipation rate can either increase or decrease.^{6,7} There is no thorough understanding of turbulence modulation by finite-size particles. It is only in the asymptotics of very small and very dilute particles that one can satisfactorily model the energy budget between the fluid and the dispersed phase. Away from these limits, either finite-size effects preclude an explicit formulation of the forces exerted on the particles or large concentrations require the understanding of possible collective effects.

Finite-size effects are usually accounted for in terms of Faxén corrections to the Stokes equation governing point-particle dynamics.^{8,9} However, it was observed¹⁰ that this approximation works only for particle whose diameters is below $\approx 4\eta$, where η designates the turbulent Kolmogorov dissipative scale. The finiteness of the particle Reynolds number becomes important at larger sizes and explicit models would require solving the full non-linear Navier-Stokes equation with the proper boundary conditions at the particle surface. A first step in tackling finite-size effects consisted in characterizing the statistics of various dynamical quantities, such as velocity, acceleration, rotation rate, for large neutrally buoyant particles in developed turbulent flows.^{11–13} One of the main findings is that average particle dynamical properties can be predicted from usual turbulent dimensional analysis at scales of the order of the particle diameter. More recently, much effort has been devoted to the characterization of the fluid flow in the vicinity of a single particle.^{14–16} In particular, it was found that it is surrounded by a boundary layer whose average thickness is of the order of its diameter. At larger distances, the influence of the particle onto the carrier fluid is negligible. Also, kinetic energy dissipation is strongly increased at the particle surface (in its viscous boundary sublayer) and weakly diminished in its wake.^{15,17}

All these observations for neutrally spherical particles were obtained in the limit where they are very dilute, so that individual disturbances of the carrier never pile up nor interfere. At higher concentrations, large particles interact together through either collisions or perturbations of the carrier flow. This “four-way coupling” occurs when particles are at distances less than the thickness of their boundary layer. In principle, if the particles are uniformly distributed in the flow with a volume fraction $\Phi_v \ll 1$, the effects of two-particles interactions are expected to be $\propto \Phi_v^2$, and are thus negligible compared to single-particle contributions which are $\propto \Phi_v$. Several works indicate that such a naive picture cannot be true. First, neutrally-buoyant particles seem to distribute in a non uniform manner; they cluster near walls^{18,19} or correlate with the large scales of the carrier flow.²⁰ It is thus probable that local particle density has strong fluctuations. Second, large particles that approach very close to each other might spend some time together. This is suggested for

instance in the simulations of Ref. 21 and could be due to strong dissipative mechanisms occurring when particles meet. This effect could lead to the creation of particle clumps, as for instance observed for heavy small-size elastic particles.²² Such collective phenomena, if exist, might be crucial in the understanding of turbulence modulation by finite-size particles.

We present here experimental results on the influence of finite-size, neutrally buoyant particles on a turbulent von Kármán flow. We find that the most noticeable effects induced by the dispersed phase is a continuous decrease of the turbulent kinetic energy and of the average inertial-range transfer rate when increasing the particle volume fraction while keeping constant the rotation speed of the impellers. We also obtain evidence that the small-scale turbulent properties of the fluid flow are unchanged by the presence of the particles. In particular, our results show surprisingly that in the presence of particles, second-order statistics of velocity increments match those of unladen flows. Finally, our results support the existence of a transition between two different regimes which occurs when the average distance between large particles is of the order of the thickness of their boundary layers.

We consider a von Kármán water flow maintained in a developed turbulent state (with $R_\lambda \approx 300$) by two impellers of diameter $d = 28$ cm that counter-rotate at an approximately constant torque. Specifically, we adjust the power of the motors at the beginning of each experiment in order to assert the same average rotational frequency of the impellers for all measurements. The enclosure has an octagonal cylindrical shape with dimensions are $40 \times 38 \times 38$ cm. The flow field is analyzed by tracking the temporal evolution of fluorescent tracer particles ($D \approx 107 \mu\text{m}$) using three cameras (Phantom V10, manufactured by Vision Research Inc., Wayne, USA) at 2900 fps. The measurement volume of approximate diameter 8 cm in the center of the tank is illuminated by a 100W laser beam. We use the weighted averaging algorithm for two-dimensional tracer finding and a “three-frames minimum acceleration” for tracking their three-dimensional trajectories.²³ The finite-size particles are super-absorbent polymer spheres whose optical index and mass density match those of water. These particles have diameters of the order of $D_p \approx 90\eta \approx L/9$, where η and L are the dissipative and integral length scales of the flow without particles. Two thin grids situated at 10 cm from the impellers prevent particles from colliding with them. This setup has been already used in Ref. 16 and 24 and more details can be found therein. We study here the fluid flow characteristics varying the volume fraction of large particles from $\Phi_v = 0$ to 10%. Each time the particle load is changed, the power of the impellers is adjusted to maintain constant their rotation frequency at $f_{\text{imp}} = 0.79$ Hz ($\pm 1.5\%$), and thus the associated Reynolds number at $Re = d^2 f_{\text{imp}}/\nu \approx 62\,000$. The different setups are summarized in Table I.

Φ_v	0	0.1%	0.3%	0.8%	2%	4%	10%
f_{imp} (Hz)	0.79	0.79	0.79	0.79	0.80	0.80	0.80
u_{rms} (m s^{-1})	0.0796	0.0797	0.0771	0.0752	0.0766	0.0578	0.0466
ε ($\text{m}^2 \text{s}^{-3}$)	0.0058	0.0055	0.0053	0.0048	0.0051	0.0032	0.0012
η (μm)	115	117	118	121	119	133	183
τ_η (ms)	13	14	14	15	14	18	33
R_λ	321	335	319	319	316	228	143

TABLE I. Characteristics of the various experiments. Φ_v volume fraction of the large particles; f_{imp} average frequency of the impellers; u_{rms} root-mean squared velocity (averaged over components); ε average kinetic energy transfer rate (measured from second-order structure function; see text); $\eta = \nu^{3/4}/\varepsilon^{1/4}$ Kolmogorov dissipative scale; $\tau_\eta = \nu^{1/2}/\varepsilon^{1/2}$ associated turnover time; R_λ Taylor-microscale Reynolds number.

We start by considering the effect of the large particles on the intensity of turbulent fluctuations. The Eulerian mean velocity profile $\langle \mathbf{u}(\mathbf{x}) \rangle$ is obtained for the different values of Φ_v by binning positions and averaging velocities over all movies. We then define velocity fluctuations as instantaneous deviations of the tracers velocity from this average field. Figure 1(a) represents the variance u_{rms}^2 of the axial (along the axis of symmetry) and transverse components of these turbulent velocity fluctuations as a function of the volume fraction of large particles. One clearly observes that the turbulent kinetic energy decreases when the particle load increases, as already observed in a different turbulent flow.⁷ Data show anisotropy, which persists for all Φ_v : the root-mean square values of axial velocity components are around 60-70% of the transverse ones. Measurements are in good agreement with $u_{\text{rms}}^2(\Phi_v) \approx u_{\text{rms}}^2(0)(1 - 3.75 \Phi_v^{2/3})$. For transverse components, one point, corresponding to $\Phi_v \approx 2\%$ clearly deviates from this form. As we will see later, this could be due to difficulties in estimating the mean flow in that case. The fitting form predicts that $u_{\text{rms}} = 0$ for $\Phi_v \gtrsim 14\%$. This could correspond to a critical volume fraction above which turbulence is completely extinguished by

the particles.

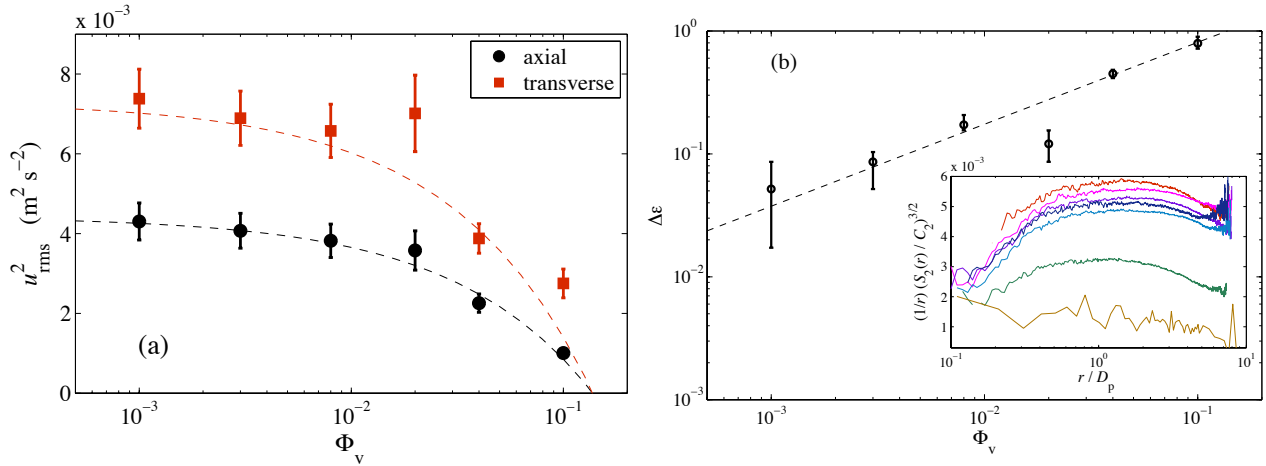


FIG. 1. (a) Variance of the turbulent velocity fluctuations $u_{\text{rms}}^2 = \langle (u_i - \langle u_i \rangle)^2 \rangle$ as a function of the particle volume fraction; The dashed lines are $u_{\text{rms}}^2(\Phi_v) = u_{\text{rms}}^2(0)(1 - 3.75\Phi_v^{2/3})$. (b) Discrepancy of the average inertial-range kinetic energy transfer rate $\Delta\epsilon = 1 - \epsilon(\Phi_v)/\epsilon(0)$ as a function of the particle volume fraction Φ_v ; the dashed line is $\Delta\epsilon = 3.75\Phi_v^{2/3}$. The rate ϵ is estimated from the inertial-range average value of the compensated second-order longitudinal velocity structure functions $S_2(r)/(C_2 r^{2/3})$ using for the Kolmogorov constant $C_2 = 2.1$. *Inset*: Dissipation rate obtained from the second-order Eulerian longitudinal structure functions for the various volume fractions (the upper curve corresponds to the case with no particles and Φ_v increases from top to bottom).

The inertial-range kinetic energy transfer rate ϵ follows a similar trend. Figure 1(b) shows that the discrepancy $\Delta\epsilon = 1 - \epsilon(\Phi_v)/\epsilon(0)$ is proportional to $\Phi_v^{2/3}$, like for the turbulent kinetic energy. Even at small values of the volume fraction, the attenuation of turbulence does not show a linear behavior $\propto \Phi_v$ (proportional to the total number of particles) that is expected if the effect of particles consists in the superposition of non-interacting individual perturbations. An attenuation $\propto \Phi_v^{2/3}$ suggests that collective effects and interactions between particles are at play. Such a scaling indicates that only a fraction of the particles have an important impact on the flow. The power two-third can be interpreted as if these active particles are located on a surface rather than in the full volume of the experiment. Several heuristic scenario can lead to such a law. First, we can imagine that particles form a given number of aggregates where all fluid flow perturbations occur in the boundary layers of the outer edge. We did not detect such aggregates in the observation volume but we cannot exclude that they are located in regions of the flow that we do not monitor (for instance close to the grids near the impellers). Recent work found that particles are likely to cluster far from the center of the von Kármán flow.²⁰ A more likely scenario relies on a kind of shielding effect where the kinetic energy is prevented from reaching the center of the flow by the particles situated at the periphery of the experiment. A full discrimination between these possibilities requires systematically scanning the entire experiment in order to measure the inhomogeneities in both the particle distribution and the fluid turbulence characteristics.

We next move to small-scale turbulent properties. A striking result is that they seem unaffected by the presence of the particles once scaled with the corresponding transfer rate ϵ , large-scale kinetic energy content u_{rms}^2 , and associated Reynolds number $R_\lambda = u_{\text{rms}}^2 \sqrt{15/(\nu\epsilon)}$. Figure 2(a) shows the second-order longitudinal Eulerian structure function of the turbulent velocity fluctuations for the various particle loading considered. All curves collapse in the inertial and sub-inertial ranges after they are represented in dissipative-scale units. In particular there are no noticeable effects (up to noise) at separations of the order of the particles diameter for Φ_v up to 10%. These results seem to contradict the kinetic energy spectra obtained in numerical simulations^{21,25} that display an enhancement of the energy contained at scales smaller than the particle size and a depletion at larger scales. These spectra are obtained from a Fourier transform of the full domain encompassing both the fluid and the particles. There are still questions whether such effects on the spectrum are inherent to the perturbed fluid flow or come from the particle velocity field. In our case, the use of Lagrangian tracers to perform Eulerian measurements isolate the fluid statistics from such pitfalls and suggest that there is no intrinsic modifications of the distribution of turbulent velocity increments by the large particles.

Statistics along tracer trajectories seem also rather insensitive to the presence of large particles. Fig-

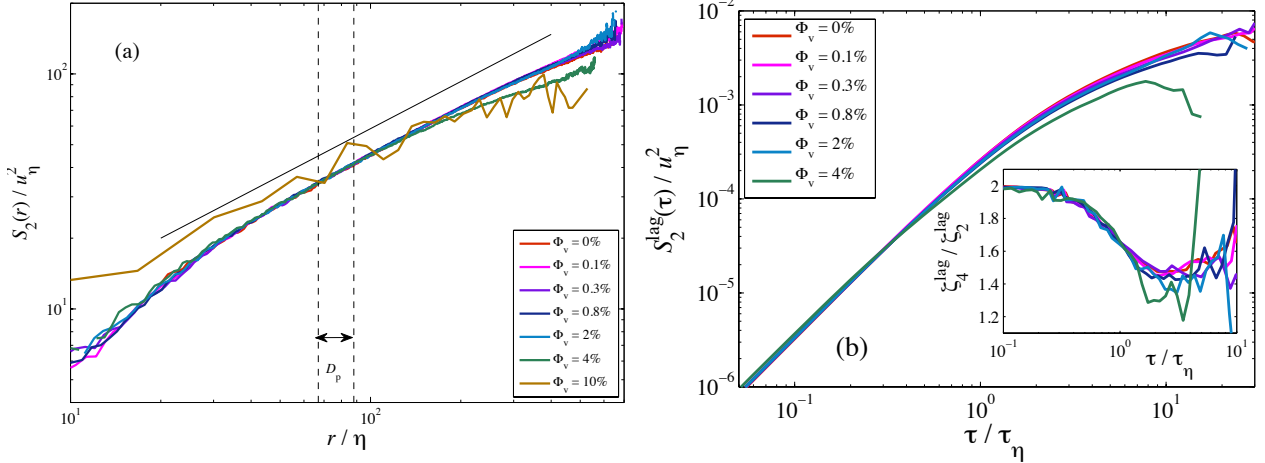


FIG. 2. (a) Second-order Eulerian longitudinal structure functions $S_2(r)$ in dissipative-range units obtained for the various values of the volume fraction Φ_v ; The solid line corresponds to a behavior $\propto r^{2/3}$; The two vertical dashed lines shows the range $54 \lesssim D_p/\eta \lesssim 88$ obtained from the maximal and minimal values of η . (b) Second-order Lagrangian structure function $S_2^{\text{lag}}(\tau)$ in dissipative-scale units. *Inset*: logarithmic derivative $(d \log S_4^{\text{lag}})/(d \log S_2^{\text{lag}})$ of the fourth-order Lagrangian structure function with respect to the second-order.

ure 2(b) shows measurements of the Lagrangian structure functions $S_p^{\text{lag}} = \langle [u_i(t + \tau) - u_i(t)]^p \rangle$, where u_i are components of the tracer velocity and the average is over the ensemble of trajectories. One observes that for $p = 2$, the collapse is not as good as for Eulerian statistics. However, Lagrangian structure functions are known to display very intermittent properties and the observed discrepancies are comparable to those obtained when comparing unladen flows at different Reynolds numbers.²⁶ We see from Tab. I that our Reynolds number decreases when the particle volume fraction increases: R_λ varies by more than a factor two when Φ_v goes from 0 to 10%. This lack of universality is not present when considering only the scaling properties through the logarithmic derivatives of the Lagrangian structure functions. For that reason, we follow Ref. 26 by showing in the inset of Fig. 2(b) the quantity $(d \log S_4^{\text{lag}})/(d \log S_2^{\text{lag}})$. Results from different volume fractions collapse to the same universal curve.

The statistics of the fluid acceleration seem also not affected by the large particles. Figure 3(a) shows the density functions of the acceleration components a_i after they are normalized by their respective second-order moments. Up to possible slight variations in the tails that could correspond to the change in Reynolds number at varying the fraction of large particles, the different curves seem to collapse reasonably well. It is known that the moments of these distributions do not reflect the actual value of the acceleration variance because of data filtering. To measure $\langle a_i^2 \rangle$ we follow the method of Voth *et al.*²⁷ consisting in extrapolating the variance when decreasing the filter size to zero. The resulting values of $a_0 = \langle a_i^2 \rangle \nu^{1/2} / \varepsilon^{3/2}$ are shown in the inset of Fig. 3(b) as a function of the Reynolds number of the flow. One clearly observes that the decrease of a_0 when Φ_v increases relates to the change in Reynolds number. Finally, the acceleration autocorrelations represented in the main panel of Fig. 3(b) are not much affected by the particle presence. The slight variations are again due to the change in Reynolds number induced by the particles.

All the quantities considered above are either reduced as $\Phi_v^{2/3}$ or not affected by the large particles. They relate to the turbulent fluctuations from which we have removed the mean flow. We actually find that the mean flow itself is strongly affected by the large-particle load. To quantify its variations as a function of the particle volume fraction, we have computed its kinetic energy large-particle load. To quantify its variations as a function of the particle volume fraction, we have computed its kinetic energy $E(\Phi_v) = \int |\langle \mathbf{u}(\mathbf{x}) \rangle|^2 d^3x$. Figure 4(a) shows that $E(\Phi_v)$ remains almost constant up to $\approx 3\%$ where it suddenly drops down. Above this critical value, the mean flow is in a different state that contains approximately twice less energy. The transition occurs roughly when the typical distance between particles becomes less than their diameter. All particles are thus necessarily feeling the presence of their neighbors through the flow modifications. This apparently has a drastic impact on the average motions as can be seen when comparing Figs. 4(b) and (c). They represents the variations of the energy and of the (x, z) components of the mean flow in the same slice of the measurement volume for $\Phi_v = 0.8\%$ (b) and 4% (c). Not only is the energy content strongly modified but also the fine structures and the directions of the mean flow. Panel (b) is representative of

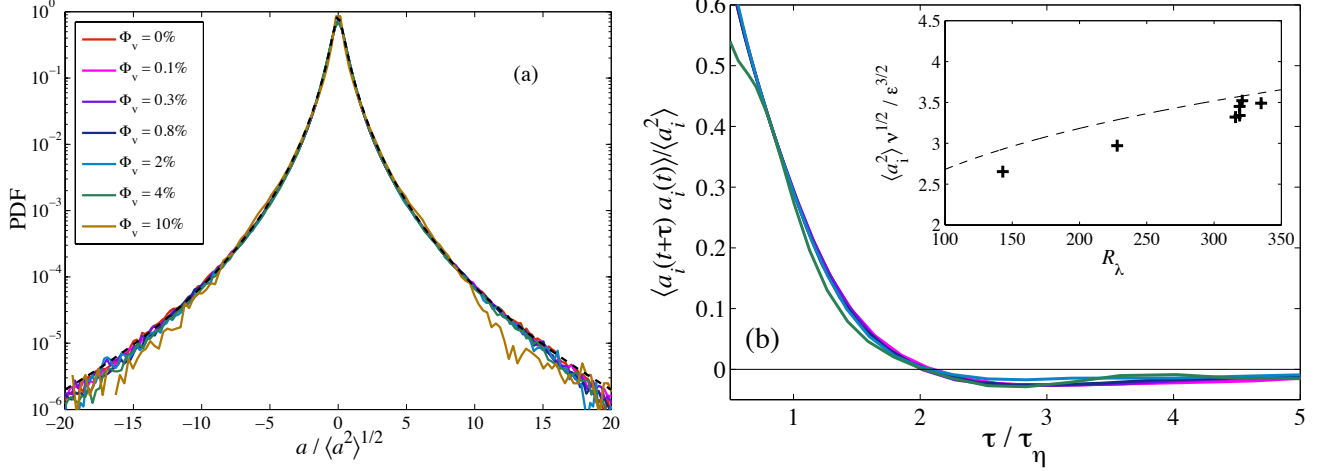


FIG. 3. (a) Normalized probability density functions of acceleration components for various values of the volume fraction Φ_v as labeled; The black dashed line is the approximative form obtained when assuming that the acceleration amplitude is log-normal.²⁸ (b) Temporal autocorrelation of the acceleration components for the same values of Φ_v . *Inset*: Normalized variance of the acceleration as a function of the Reynolds number R_λ ; Each symbol is a different experiment and the dashed line is the fit proposed by Hill²⁹ for the intermittent dependence of the acceleration variance as a function of R_λ .

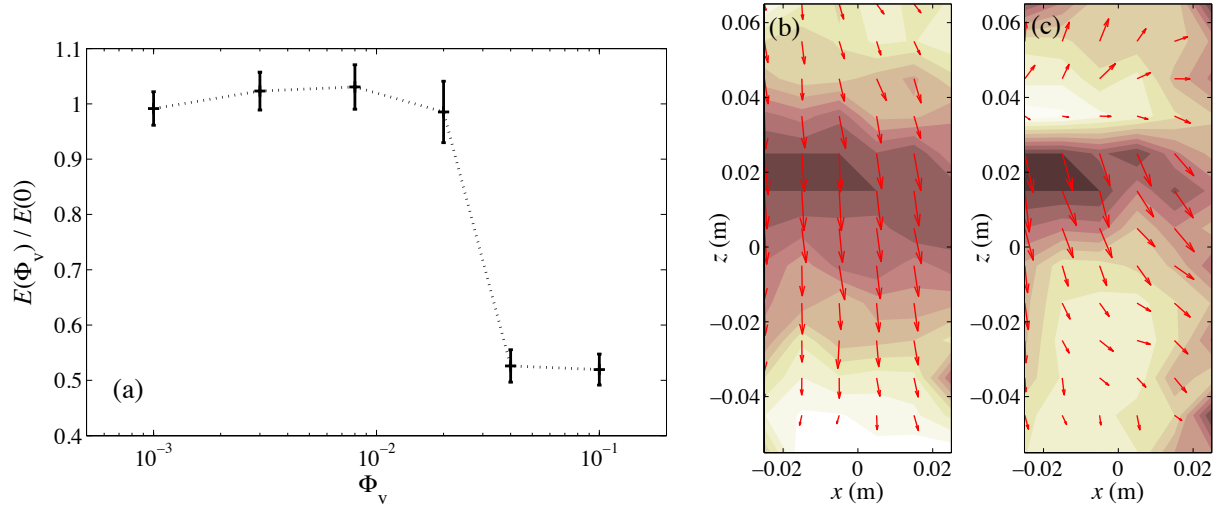


FIG. 4. (a) Mean flow kinetic energy $E(\Phi_v)$ contained in the measurement volume as a function of the large-particle volume fraction. (b) and (c) Slice of the mean flow in a central part of the measurement volume for $\Phi_v = 0.8\%$ and 4% , respectively (the x direction is along the impellers axis of rotation). The colored background shows the velocity squared modulus (normalized in each case to its mean; increasing values from white to black) and the arrows show the (x, z) components of the velocity field.

all volume fractions below 0.8% while panel (c) is also representative of $\Phi_v = 10\%$. For $\Phi_v = 2\%$, the mean flow obtained when time-averaging is very different from these two states. We however suspect it to be non stationary because several movies show extremely strong deviations from the mean. Unfortunately, our experiment was conceived to focus on small-scale turbulent properties and not designed to accurately measure large scale variations. A better understanding of what is happening for this volume fraction would require revisiting our setup in order to focus on the large scales. This would also allow us a more accurate study of a possible phase transition for Φ_v of the order of a few percents.

To conclude, let us stress again our main findings on the modification of a turbulent von Kármán flow by finite-size neutrally-buoyant spherical particles. The most surprising result is that inertial-range and small-scale turbulent features are unchanged in the presence of particles for volume fractions up to $\Phi_v = 10\%$. There is no signature of the particle size and its associated timescale neither on the scaling properties of the

fluid turbulent velocity fluctuations nor on the statistics of the acceleration. The only noticeable effects are on global quantities. In our specific setup and when the impeller rotation rate is maintained, the turbulent kinetic energy and the inertial-range transfer rate of the bulk flow are continuously decreasing when the particle volume fraction is increased. However, our setup does not monitor the energy injection rate. We are thus unable to discriminate between a decrease of the power needed to maintain the impellers rotation speed (i.e. a sort of drag reduction) and a redistribution of the energy dissipation to the regions closer to the impellers (outside of our observation volume). A better understanding would require a more accurate handling of the impeller torque and thorough measurements of the fluid velocity in the full experimental domain. Such measures could clarify the possible phase transition at $\Phi_v \approx 3\%$. In particular, they would allow us to draw differences between what is due to the specificities of von Kármán inhomogeneous flow and a possible universal change at such volume fractions in the coupling between the turbulent flow and the particles.

This research has received funding from the European Research Council under the European Community's Seventh Framework Program (FP7/2007-2013 Grant Agreement No. 240579) and from the French Agence Nationale de la Recherche (Programme Blanc ANR-12-BS09-011-04).

- ¹C. M. White and M. G. Mungal, "Mechanics and prediction of turbulent drag reduction with polymer additives," *Annu. Rev. Fluid Mech.* **40**, 235–256 (2008).
- ²P. Perlekar, D. Mitra, and R. Pandit, "Manifestations of drag reduction by polymer additives in decaying, homogeneous, isotropic turbulence," *Phys. Rev. Lett.* **97**, 264501.1–264501.4 (2006).
- ³S. Balachandar and J. K. Eaton, "Turbulent dispersed multiphase flow," *Annu. Rev. Fluid Mech.* **42**, 111–133 (2010).
- ⁴J.-P. Matas, J. F. Morris, and E. Guazzelli, "Transition to turbulence in particulate pipe flow," *Phys. Rev. Lett.* **90**, 014501 (2003).
- ⁵V. Loisel, M. Abbas, O. Masbernat, and E. Climent, "The effect of neutrally buoyant finite-size particles on channel flows in the laminar-turbulent transition regime," *Phys. Fluids* **25**, 123304 (2013).
- ⁶F. Lucci, A. Ferrante, and S. Elghobashi, "Modulation of isotropic turbulence by particles of Taylor length-scale size," *J. Fluid Mech.* **650**, 5–55 (2010).
- ⁷G. Bellani, M. L. Byron, A. G. Collignon, C. R. Meyer, and E. A. Variano, "Shape effects on turbulent modulation by large nearly neutrally buoyant particles," *J. Fluid Mech.* **712**, 41–60 (2012).
- ⁸R. Gatignol, "The Faxén formulae for a rigid sphere in an unsteady non-uniform Stokes flow," *J. Méc. Théor. Appl.* **1**, 143–160 (1983).
- ⁹M. Maxey and J. Riley, "Equation of motion for a small rigid sphere in a nonuniform flow," *Phys. Fluids* **26**, 883–889 (1983).
- ¹⁰H. Homann and J. Bec, "Finite-size effects in the dynamics of neutrally buoyant particles in turbulent flow," *J. Fluid Mech.* **651**, 81 (2010).
- ¹¹N. Qureshi, M. Bourgoin, C. Baudet, A. Cartellier, and Y. Gagne, "Turbulent transport of material particles: an experimental study of finite size effects," *Phys. Rev. Lett.* **99**, 184502 (2007).
- ¹²H. Xu and E. Bodenschatz, "Motion of inertial particles with sizes larger than Kolmogorov scales in turbulent flows," *Physica D* **237**, 2095–2100 (2008).
- ¹³R. Zimmermann, Y. Gasteuil, M. Bourgoin, R. Volk, A. Pumir, and J.-F. Pinton, "Rotational intermittency and turbulence induced lift experienced by large particles in a turbulent flow," *Phys. Rev. Lett.* **106**, 154501 (2011).
- ¹⁴G. Bellani and E. A. Variano, "Slip velocity of large neutrally buoyant particles in turbulent flows," *New J. Phys.* **14**, 125009 (2012).
- ¹⁵M. Cisse, H. Homann, and J. Bec, "Slipping motion of large neutrally buoyant particles in turbulence," *J. Fluid Mech.* **735**, R1 (2013).
- ¹⁶S. Klein, M. Gibert, A. Bérut, and E. Bodenschatz, "Simultaneous 3D measurement of the translation and rotation of finite-size particles and the flow field in a fully developed turbulent water flow," *Meas. Sci. Technol.* **24**, 024006 (2013).
- ¹⁷T. Tanaka and J. K. Eaton, "Sub-Kolmogorov resolution particle image velocimetry measurements of particle-laden forced turbulence," *J. Fluid Mech.* **643**, 177–206 (2010).
- ¹⁸B. Chun and A. Ladd, "Inertial migration of neutrally buoyant particles in a square duct: An investigation of multiple equilibrium positions," *Phys. Fluids* **18**, 031704 (2006).
- ¹⁹A. G. Kidanemariam, C. Chan-Braun, T. Doychev, and M. Uhlmann, "Direct numerical simulation of horizontal open channel flow with finite-size, heavy particles at low solid volume fraction," *New J. Phys.* **15**, 025031 (2013).
- ²⁰N. Machicoane, R. Zimmermann, L. Fiabane, M. Bourgoin, J.-F. Pinton, and R. Volk, "Large sphere motion in a nonhomogeneous turbulent flow," *New J. Phys.* **16**, 013053 (2014).
- ²¹A. Ten Cate, J. Dersksen, L. Portela, and H. van den Akker, "Fully resolved simulations of colliding monodisperse spheres in forced isotropic turbulence," *J. Fluid Mech.* **519**, 233–271 (2004).
- ²²J. Bec, S. Musacchio, and S. S. Ray, "Sticky elastic collisions," *Phys. Rev. E* **87**, 063013 (2013).
- ²³N. T. Ouellette, H. Xu, and E. Bodenschatz, "A quantitative study of three-dimensional lagrangian particle tracking algorithms," *Exp. Fluids* **40**, 301–313 (2006).
- ²⁴S. Klein, "Dynamics of large particles in turbulence," (2012), diplomarbeit.
- ²⁵K. Yeo, S. Dong, E. Climent, and M. Maxey, "Modulation of homogeneous turbulence seeded with finite size bubbles or particles," *Int. J. Multiphase Flow* **36**, 221 – 233 (2010).
- ²⁶L. Biferale, E. Bodenschatz, M. Cencini, A. S. Lanotte, N. T. Ouellette, F. Toschi, and H. Xu, "Lagrangian structure functions in turbulence: A quantitative comparison between experiment and direct numerical simulation," *Phys. Fluids* **20**, 065103 (2008).
- ²⁷G. Voth, A. La Porta, A. Crawford, and E. Bodenschatz, "Measurement of particle accelerations in fully developed turbulence," *J. Fluid Mech.* **469**, 121–160 (2002).

- ²⁸N. Mordant, A. M. Crawford, and E. Bodenschatz, “Three-dimensional structure of the lagrangian acceleration in turbulent flows,” *Phys. Rev. Lett.* **93**, 214501 (2004).
- ²⁹R. J. Hill, “Scaling of acceleration in locally isotropic turbulence,” *J. Fluid Mech.* **452**, 361–370 (2002).